High Performance Soft X-Ray RIXS and Applications to Magnetic Materials

Jun Miyawaki

Institute for Solid State Physics, The University of Tokyo

11th International Conference on Inelastic X-ray Scattering (IXS2019)
Charles B. Wang Center, Stony Brook University, New York, USA, June 23–28, 2019

Outline

- RIXS-MCD at HORNET

  J. Miyawaki *et al.*, J. Synchrotron Rad. **24**, 449–455 (2017).

  J. Miyawaki *et al.*, PRB **96**, 214420 (2017).

  R. Y. Umetsu *et al.*, PRB **99**, 134414 (2019).

- Two new RIXS beamlines in New 3 GeV Ring at Tohoku, Japan

RIXS-MCD at HORNET

HORNET station

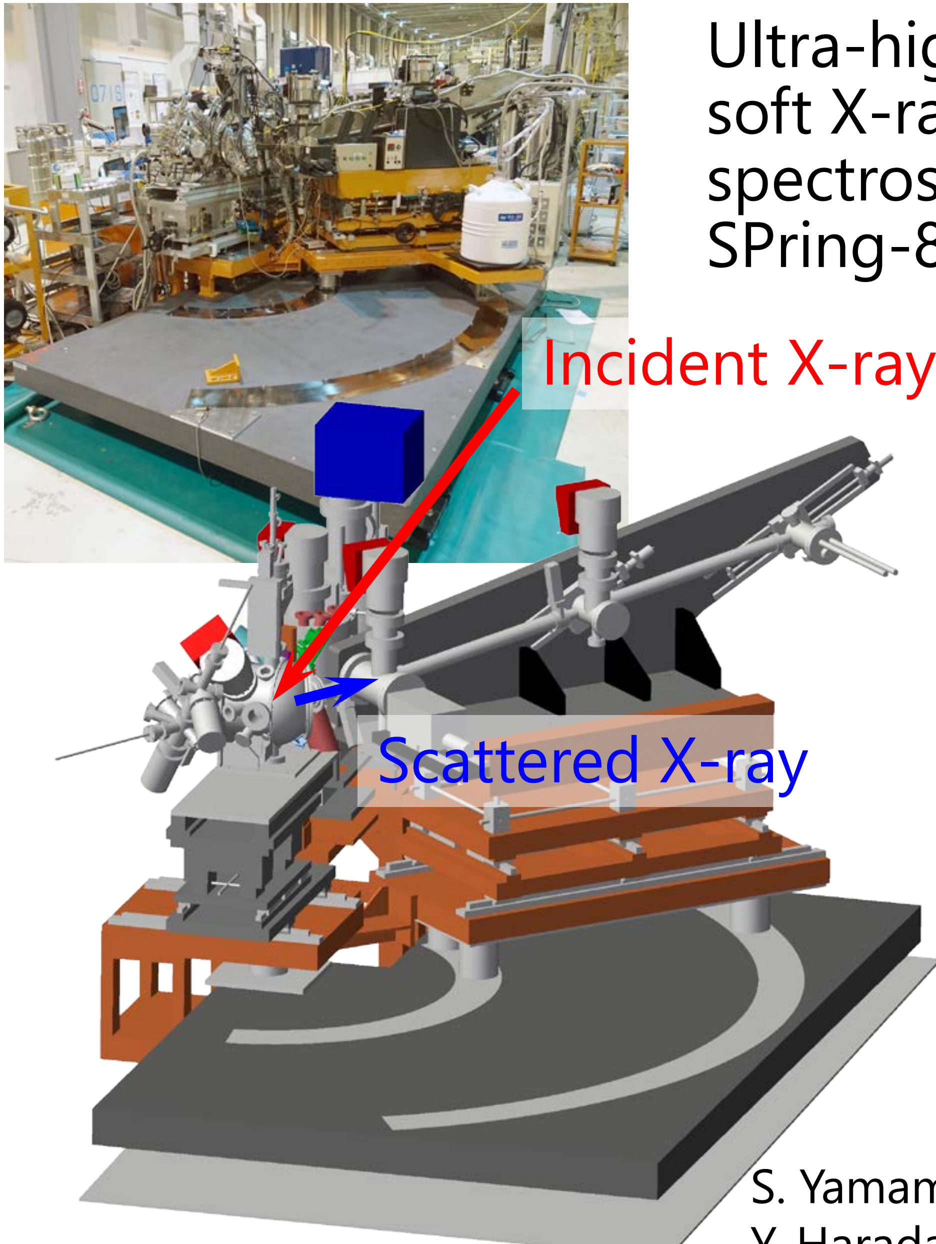

Ultra-high resolution soft X-ray emission spectroscopy station (HORNET), SPring-8 BL07LSU

Specifications

- Energy Range
  BL: 250–2000 eV
  Spectrometer: 350–750 eV
- Polarization
  Linear(Horizontal/Vertical)
  Circular (Left and Right)
- Beam Size
  v: 5 µm x h: 30 µm
- Total Energy Resolution
  < 220 meV@710 eV

S. Yamamoto *et al.*, J. Synchrotron Rad. **21**, 352 (2014).
Y. Harada *et al.*, Rev. Sci. Instrum. **83**, 013116 (2012).

RIXS in Magnetic Field

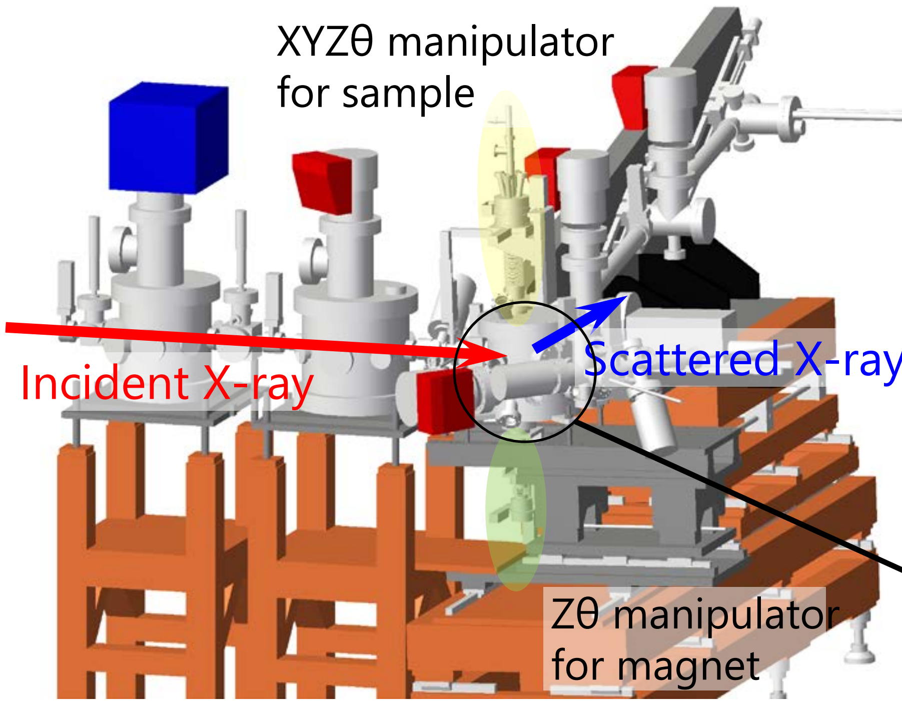

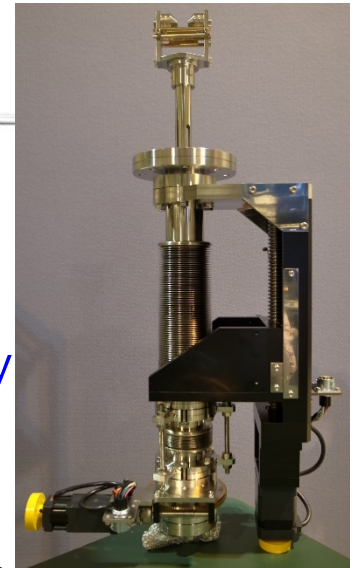

Hole for X-ray

Magnetic circuit composed of
Neodymium magnet and Yoke

Magnetic field ＞ 0.25 T

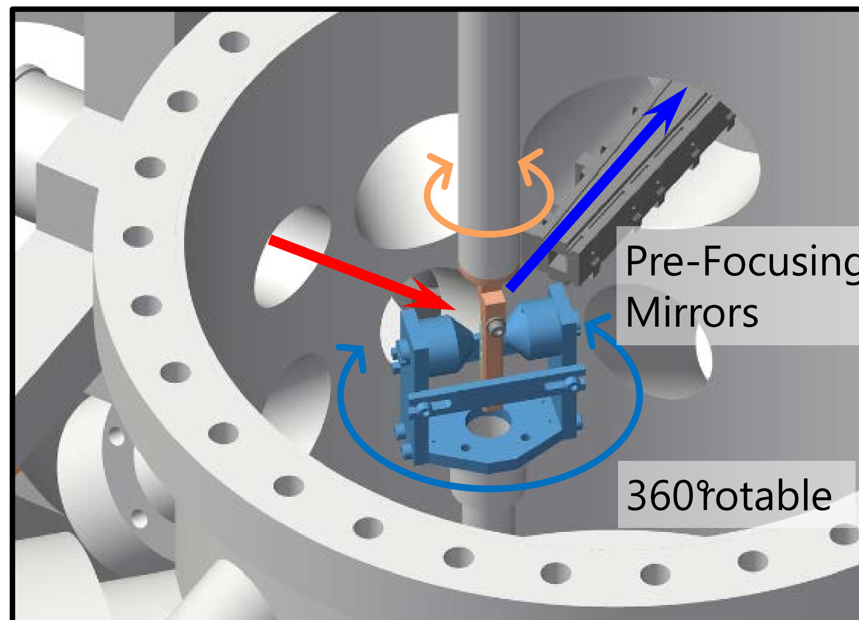

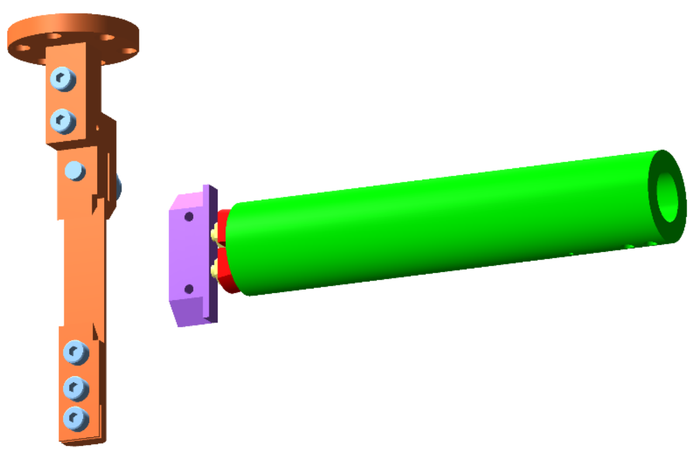

Dedicated Sample Transfer System

J. Miyawaki *et al.*, J. Synchrotron Rad. **24**, 449 (2017).

Application of RIXS-MCD

Weakferromagnet α-Fe_2O_3 J. Miyawaki *et al.*, PRB **96**, 214420 (2017).

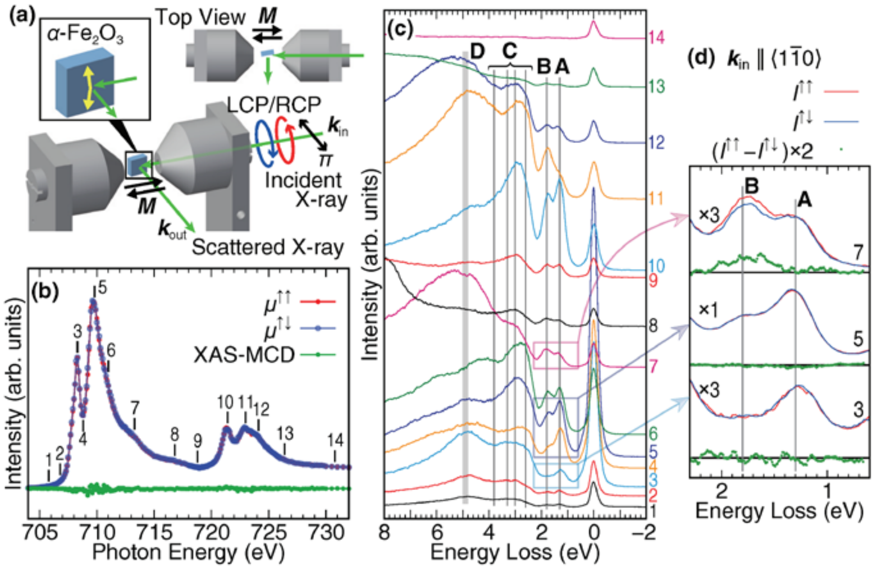

Half-metal CrO_2 H. Fujiwara *et al.*

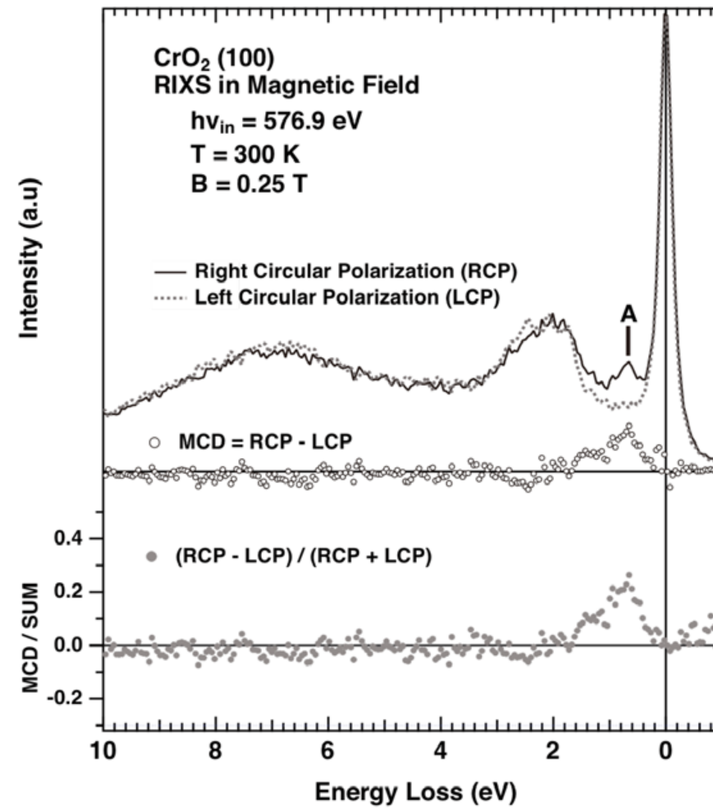

Half-metal-type Heusler alloy Mn_2VAl

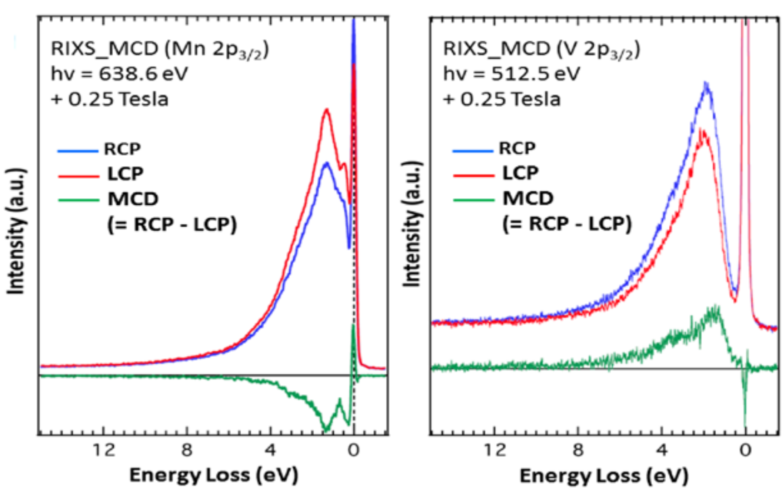

R. Y. Umetsu *et al.*, PRB **99**, 134414 (2019).

Crystal Structure and Magnetism of α-Fe_2O_3

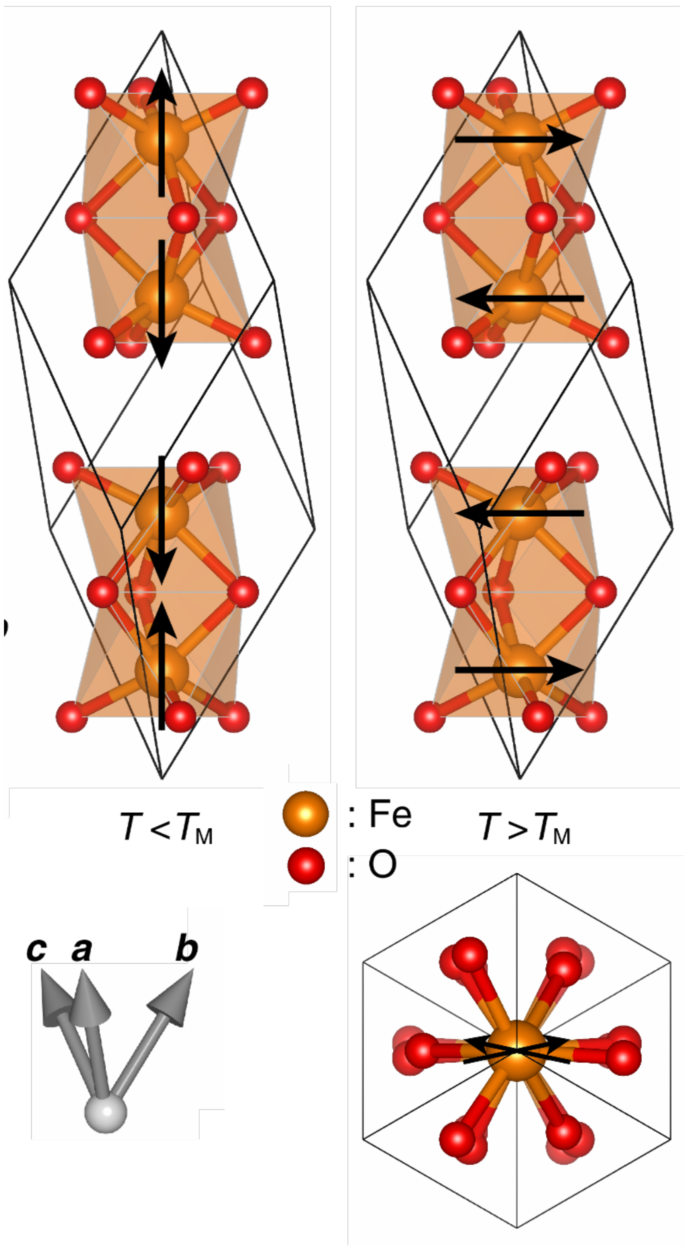

Crystal Structure

corundum structure

rhombohedral (hexagonal) unit cell

Magnetism

Néel temperature: $T_N \approx 950$ K

Morin transition temperature: $T_M \approx 250$ K

$T > 250$ K: canted antiferromagnetic, M⊥[111]

$T < 250$ K: uniaxial antiferromagnetic, M∥ [111]

- A prototype material of the Dzyaloshinskii-Moriya interaction (DMI)
- Showing **weak ferromagnetism** due to DMI

XMLD and XMCD of α-Fe_2O_3

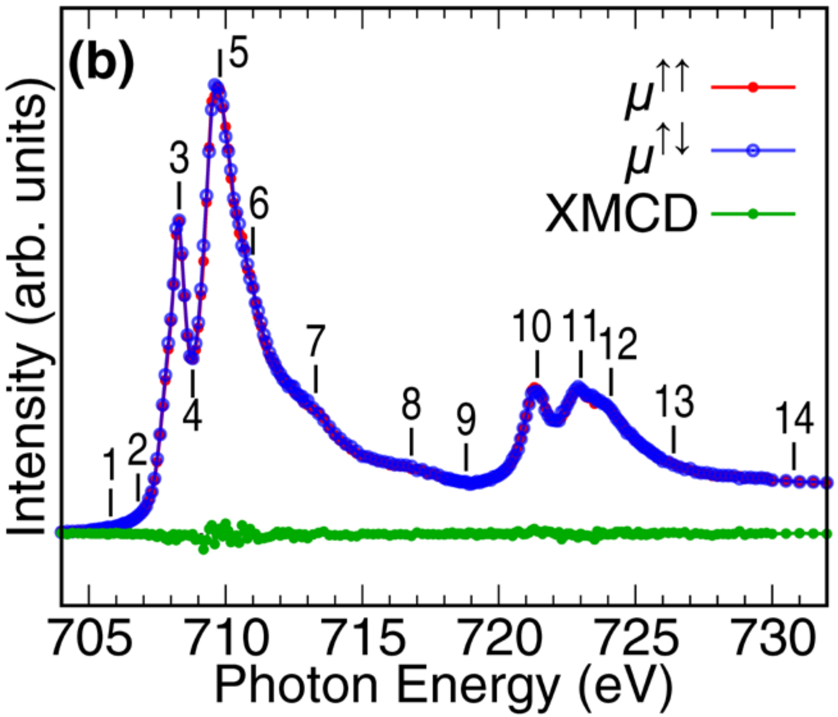

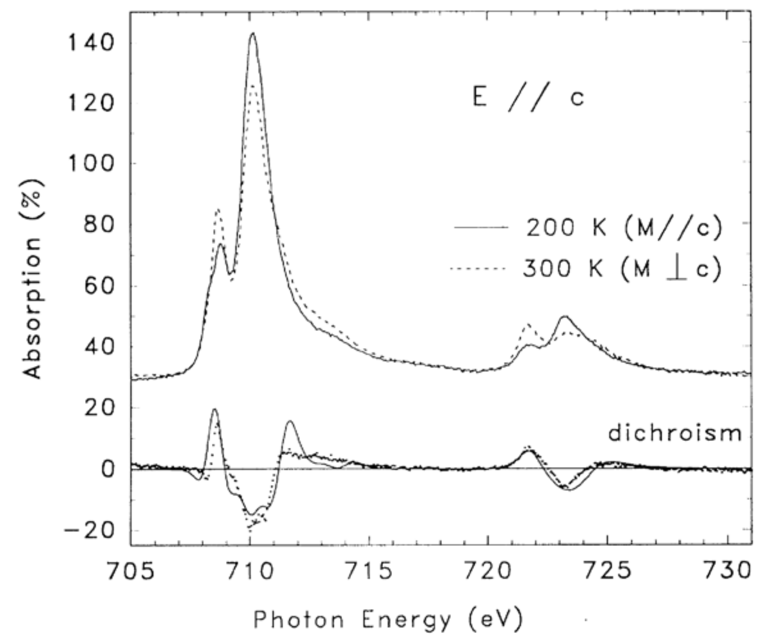

P. Kuiper *et al.*, PRL **70**, 1549 (1993).

No discernible XMCD was observed.

XMLD revealed the orientation of the magnetic moment.

Motivation

Identifying the electronic structure inducing the weak ferromagnetism in α-Fe_2O_3 by DMI and revealing its mechanism by RIXS-MCD.

Crystal Orientation & Excitation Energy Dependence

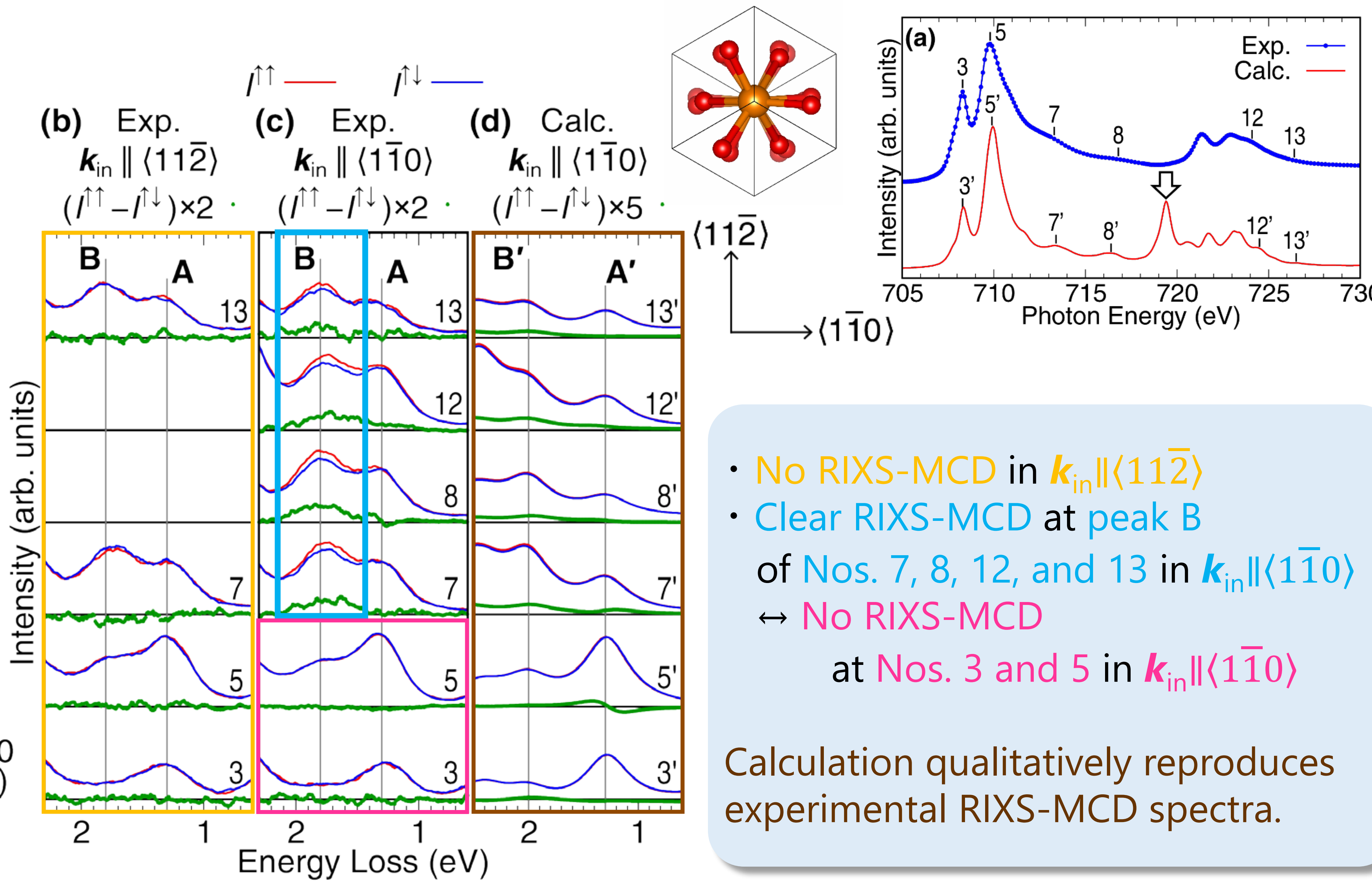

- No RIXS-MCD in $\boldsymbol{k}_{\mathrm{in}} \parallel \langle 11\bar{2}\rangle$
- Clear RIXS-MCD at peak B of Nos. 7, 8, 12, and 13 in $\boldsymbol{k}_{\mathrm{in}} \parallel \langle 1\bar{1}0\rangle$
  ↔ No RIXS-MCD at Nos. 3 and 5 in $\boldsymbol{k}_{\mathrm{in}} \parallel \langle 1\bar{1}0\rangle$

Calculation qualitatively reproduces experimental RIXS-MCD spectra.

Origin of RIXS-MCD in α-Fe_2O_3

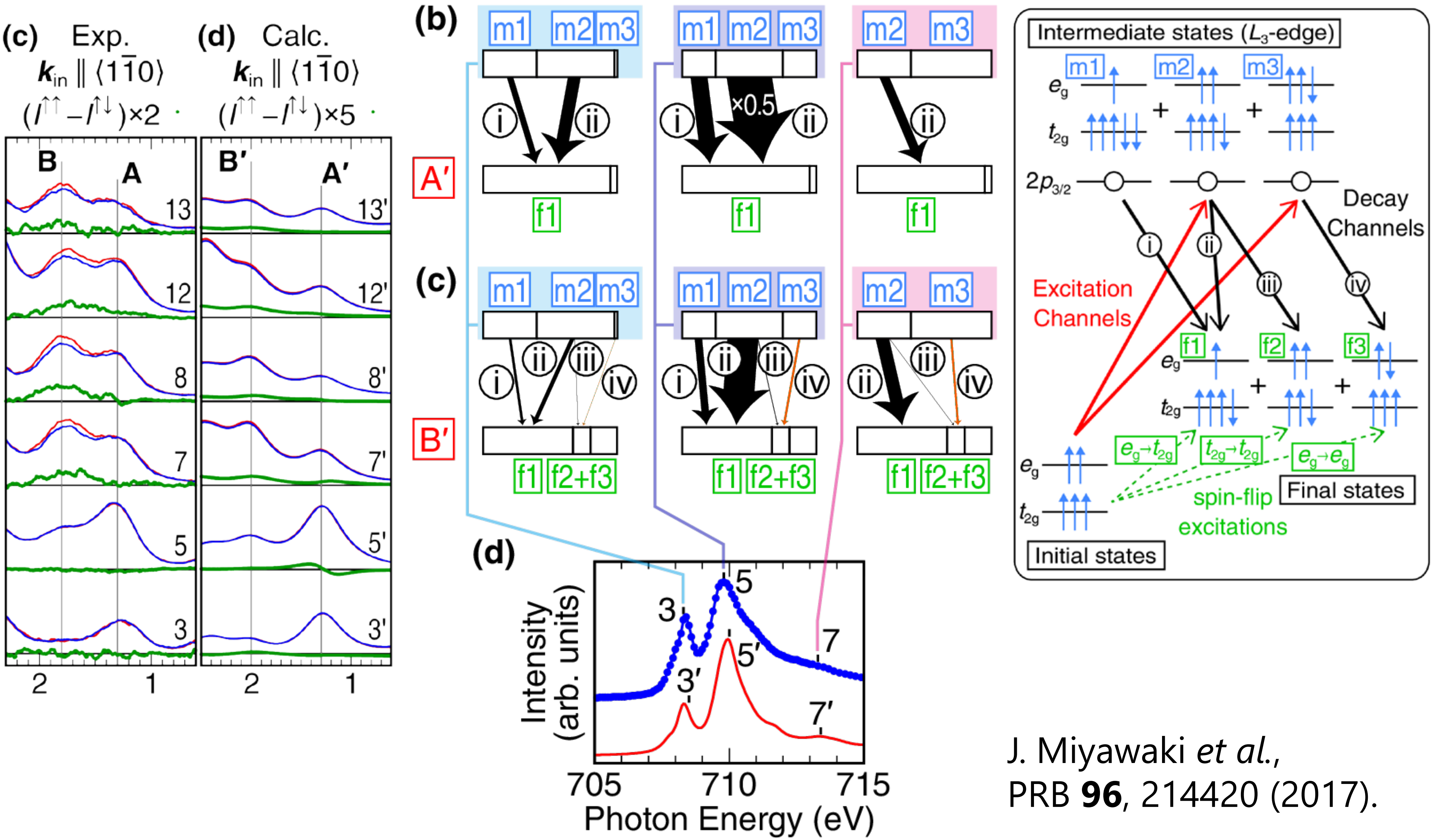

J. Miyawaki *et al.*,
PRB **96**, 214420 (2017).

RIXS-MCD originates from ***$e_g \rightarrow e_g$* spin-flip excitation**.

Mn_2VAl : $L2_1$-ordered Heusler alloy

Ferrimagnetism (Tc = 750 K) [1]

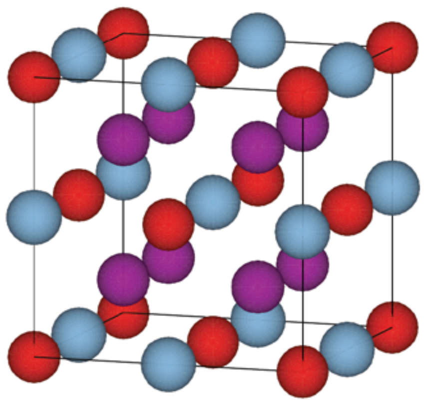

L21-ordered
Heusler Alloy
a = 5.68 Å [2,3]
Space group:
Fm-3m (No. 225)

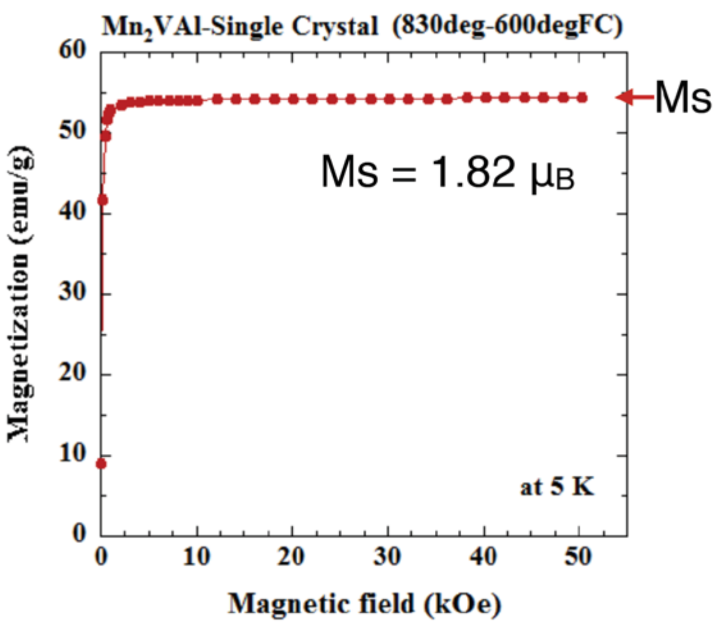

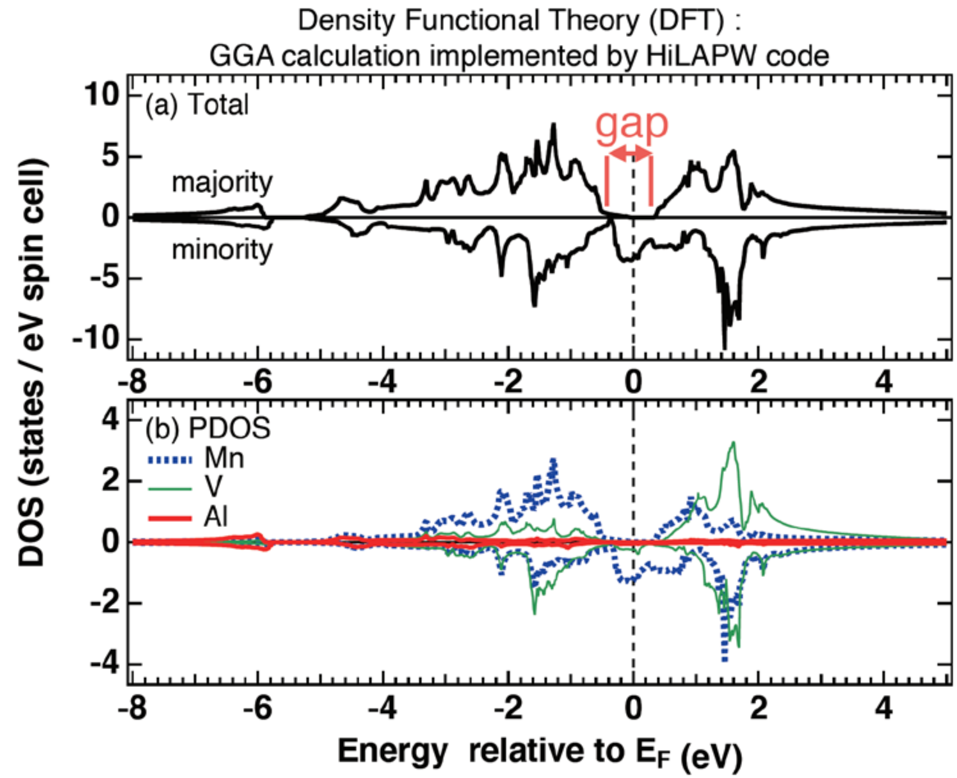

- Predicted "half-metal" type electronic structures
- Saturation Magnetization is smaller than that for Co-based Heusler alloy (Ms ~5 μ_B) [4].

  Current driven Magnetization switching : $I_{switch} \propto Ms^2$

[1] Y. Yoshida M. Kawakami, and T. Nakamichi: J. Phys. Soc. Jpn. **50**, 2203 (1981).
[2] T. Kubota *et al.* Appl. Phys. Lett. **95**, 222503 (2009).
[2] K. Momma and F. Izumi, J. Appl. Crystallogr., 44, 1272-1276 (2011).
[4] C. Jiang *et al.*, Solid State Commun. **118**, 513 (2001).

RIXS-MCD of Mn_2VAl

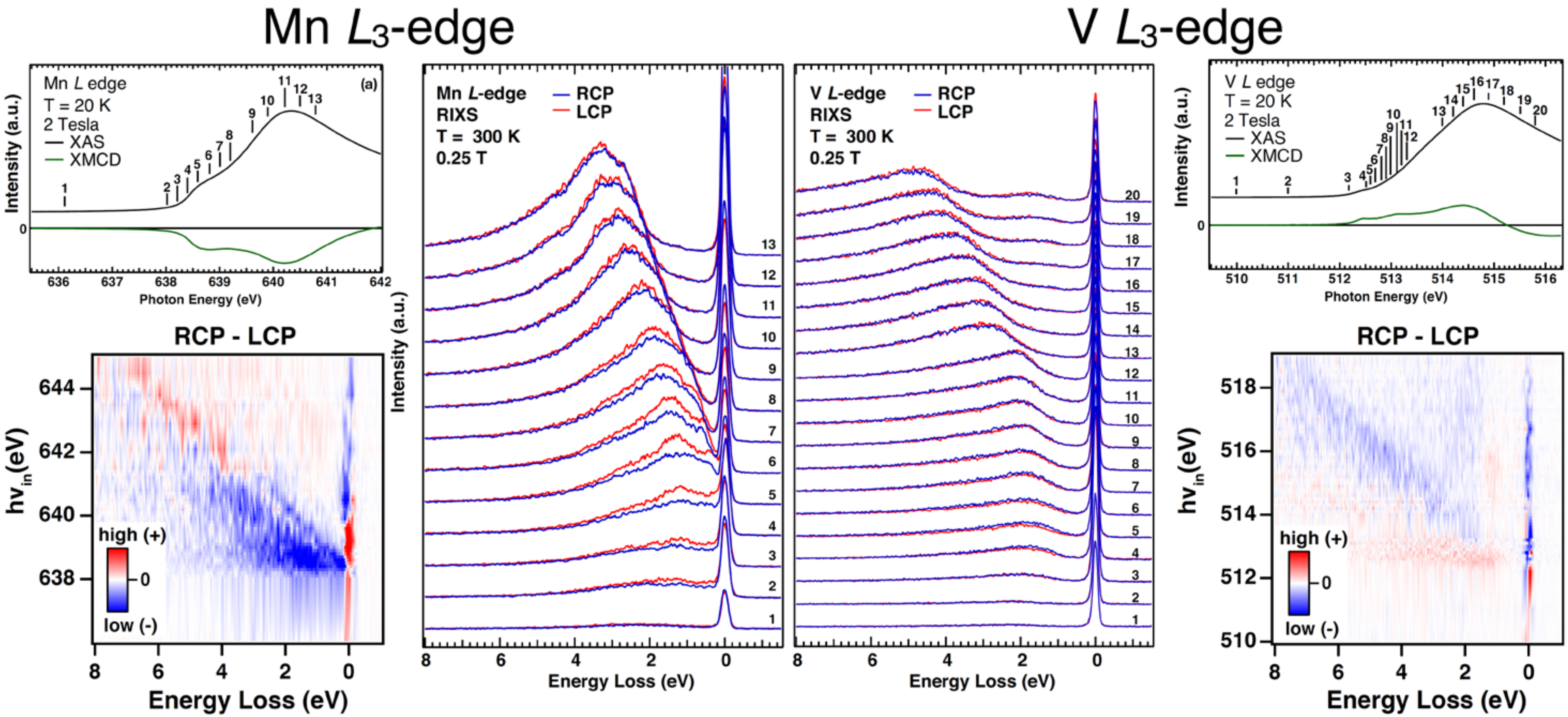

RIXS-MCD was clearly observed at the Mn L_3 pre-edge.

Spectral simulation: *hν*-dependence

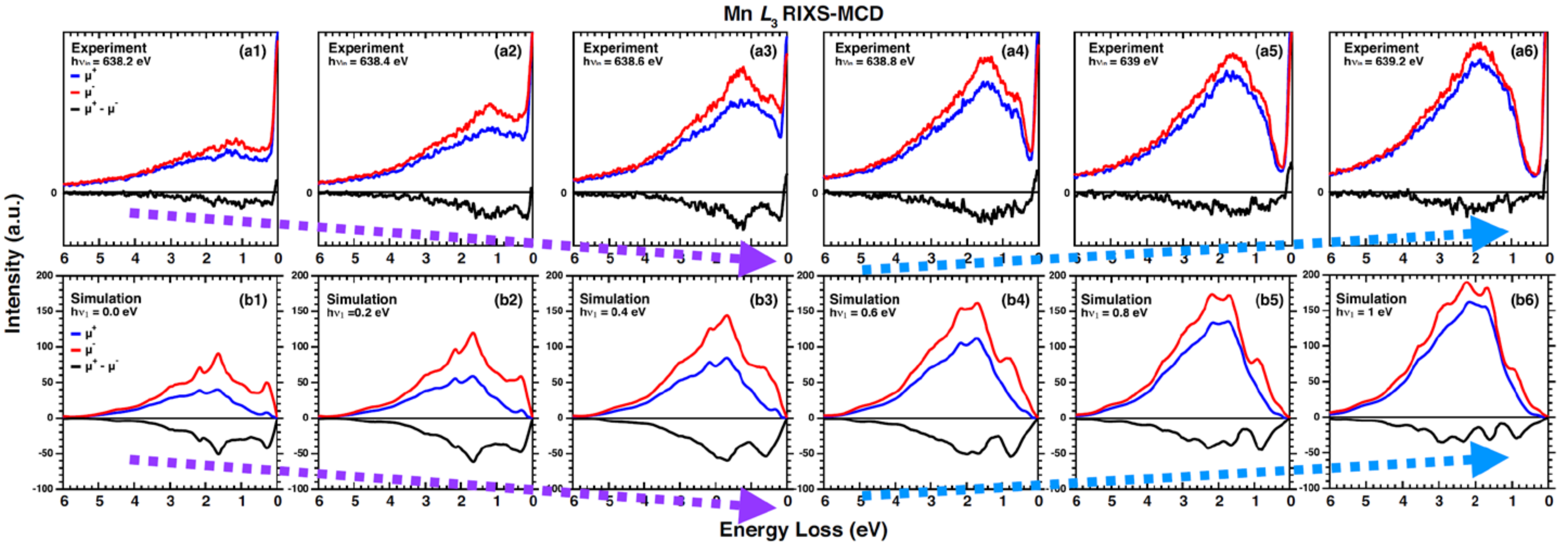

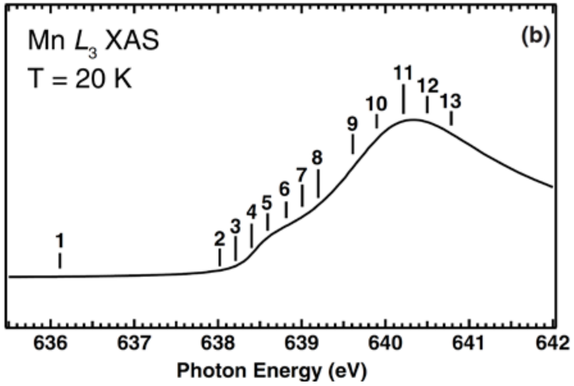

Spectral simulations have successfully explained the experimental RXES-MCD spectra.

Probing spin-polarized electronic structure

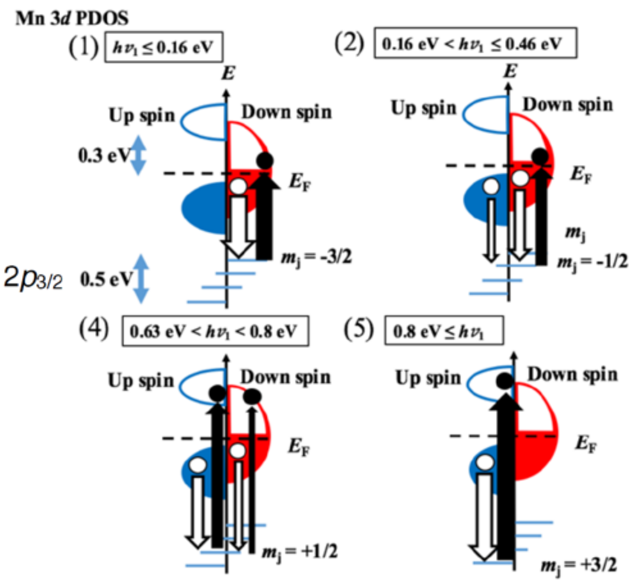

m_j	eV
-3/2	0
-1/2	-0.16
+1/2	-0.33
+3/2	-0.50

Zeeman splitting
2p (j =3/2) states

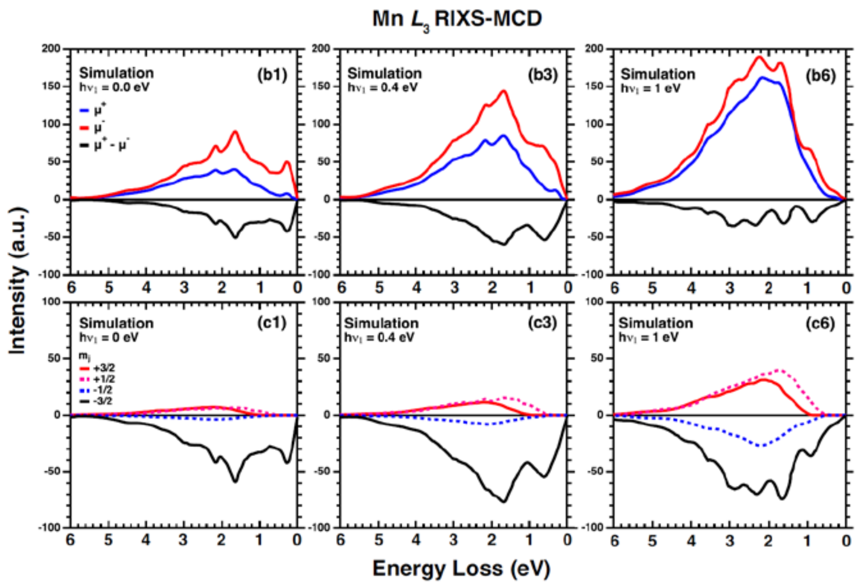

- ✓ 2*p* core states lifts the degeneracy
  by the effective magnetic field due to the 3*d* states.
- ✓ The low $h\nu_{in}$ emission mainly comes from the de-exciation to the fully spin-polarized $2p_{3/2}$ $m_j = -3/2$ states, which allows us to probe the spin-polarized electronic structures

Two New RIXS Beamlines
in New 3 GeV Ring at Tohoku

New 3 GeV Ring at Tohoku, Japan

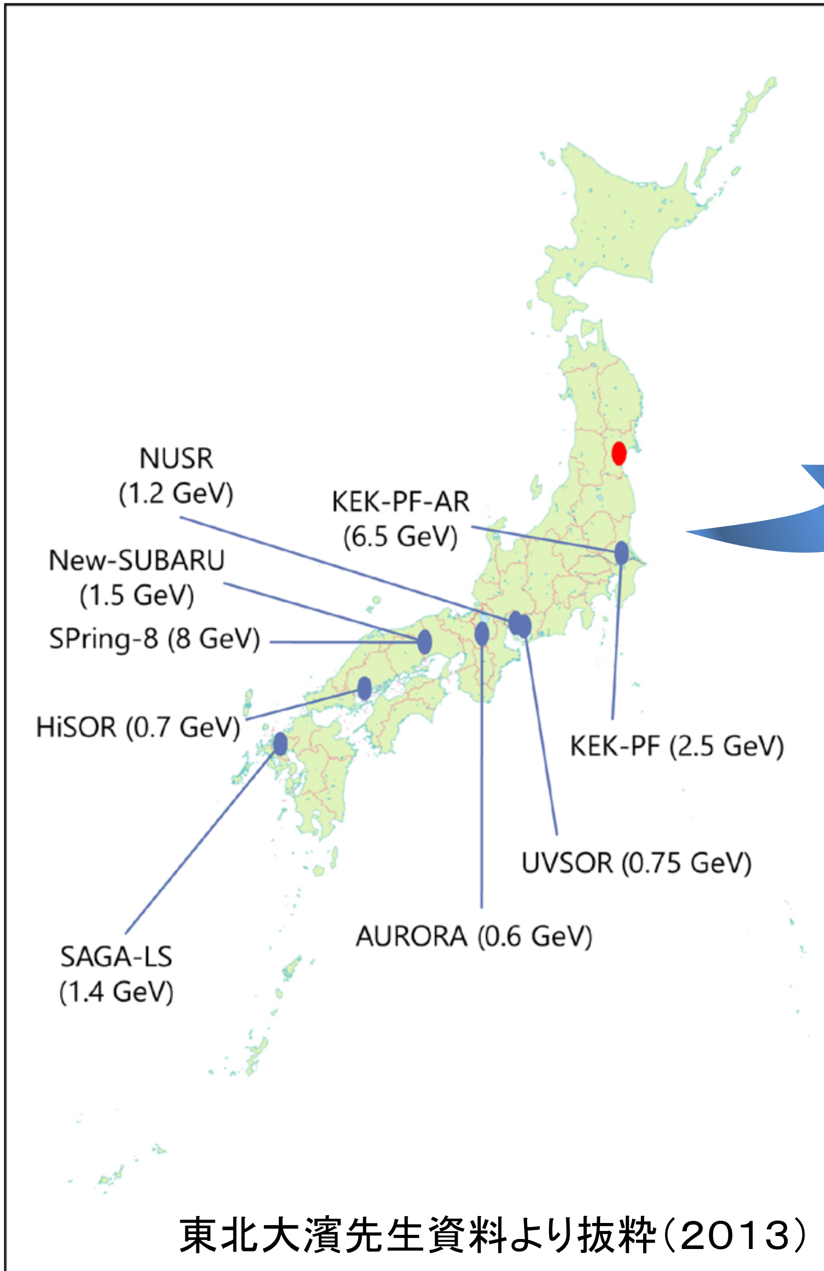

The construction of a next-generation 3 GeV light source has just started in Tohoku Sendai, Japan.
The 1st light is scheduled late in 2023.

New 3 GeV Ring at Tohoku, Japan

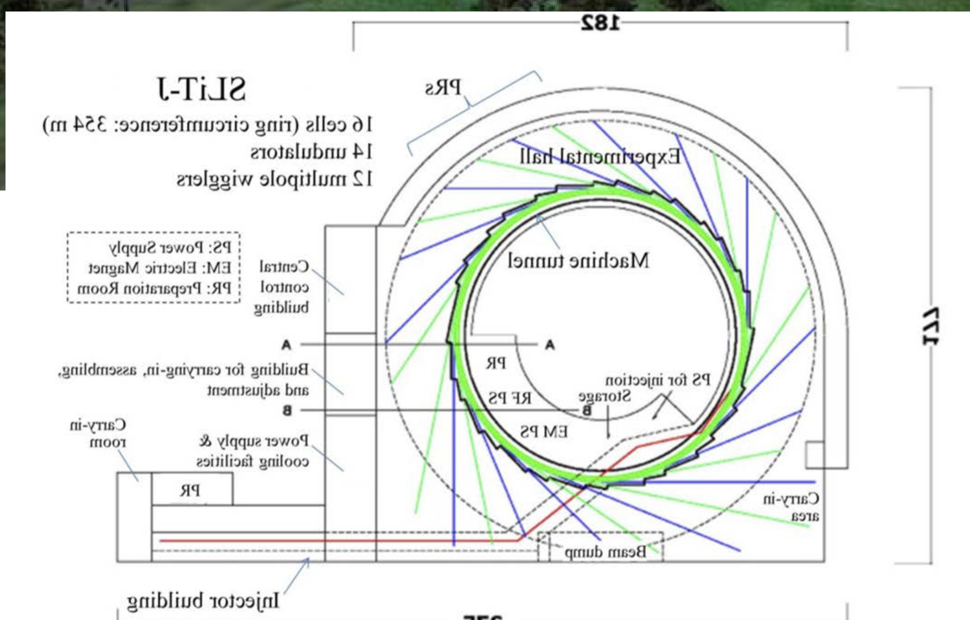

Concept Design Report ver2.1 (May, 2016)
http://www.slitj.tagen.tohoku.ac.jp/outline/technology.html

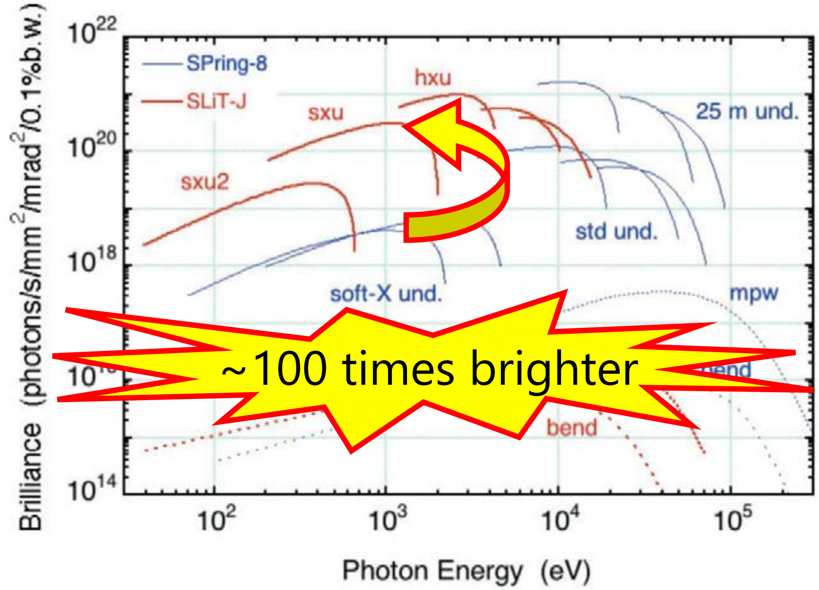

Ring	
Beam energy (GeV)	2.998
Beam current (mA)	400
Natural emittance (nmrad)	0.93
β_x, β_y, η_x at long straight section	13.0, 3.0, 0.0
Natural energy spread	0.082%
σ_x (μm)	110
σ_y (μm)	2.4
$\sigma_{x'}$ (μrad)	8.45
$\sigma_{y'}$ (μrad)	0.79
ID	
Period length (mm)	56
Number of periods	75
Total length (m)	4.2
Energy range (eV)	200–1500

Upgrade of HORNET

Parameters

Present HORNET

Δ_S=**5 µm**, Δ_{SE}=**0.2 µrad** in rms, and Δ_D=**24 µm**, k=1, γ=18°, a_0=2200 l/mm

HE grating

R=16268 mm, a_1=0.603147 l/mm^2, a_2=−3.11735×10^{-3} l/mm^3, a_3=8.99359×10^{-6} l/mm^4

LE grating

R=16268 mm, a_1=0.603147 l/mm^2, a_2=−2.24449×10^{-3} l/mm^3, a_3=8.99359×10^{-6} l/mm^4

r_1 and α are optimized.

Upgraded HORNET

Δ_S=**0.5 µm**, Δ_{SE}=**0.1 µrad** in rms, and Δ_D=**5 µm**, k=1, γ=18°, a_0=2200 l/mm,

HE grating (optimized at E_0=700 eV, r_1=505.0 mm, r_2=1917.7 mm, α=87.3°)

R=17560.0 mm, a_1=0.693643 l/mm^2, a_2=−3.10053×10^{-3} l/mm^3, a_3=9.73493×10^{-6} l/mm^4

LE grating (optimized at E_0=450 eV, r_1=550.0 mm, r_2=2029 mm, α=87.5°)

R=20036.0 mm, a_1=0.824049 l/mm^2, a_2=−1.01424×10^{-3} l/mm^3, a_3=4.29688×10^{-6} l/mm^4

r_1 and α are optimized.

Present vs Upgrade

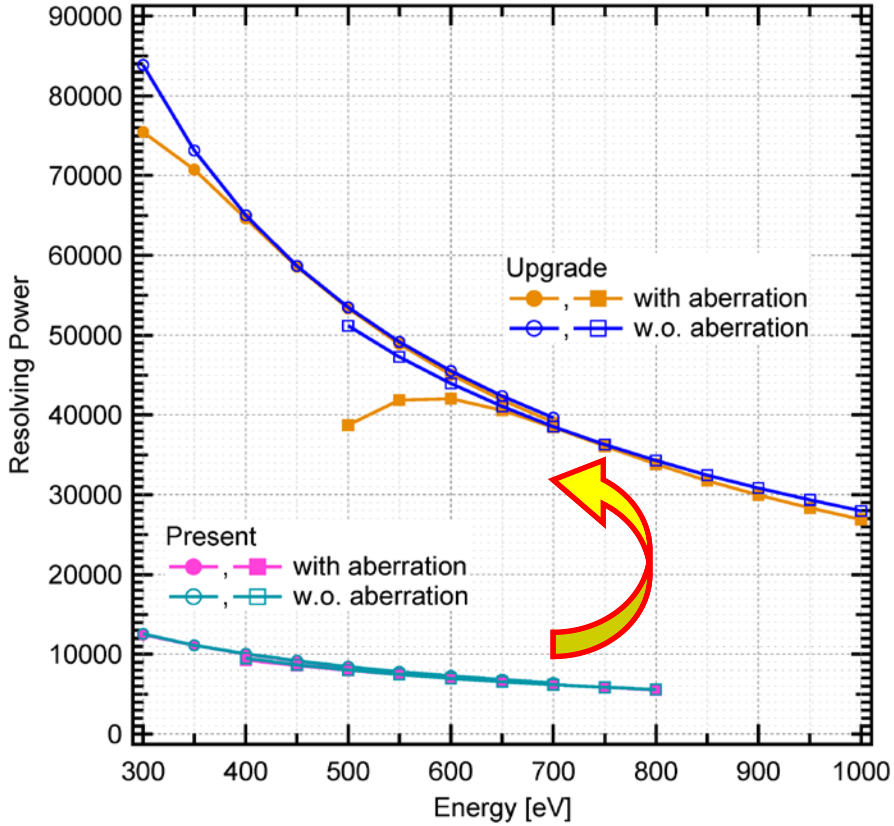

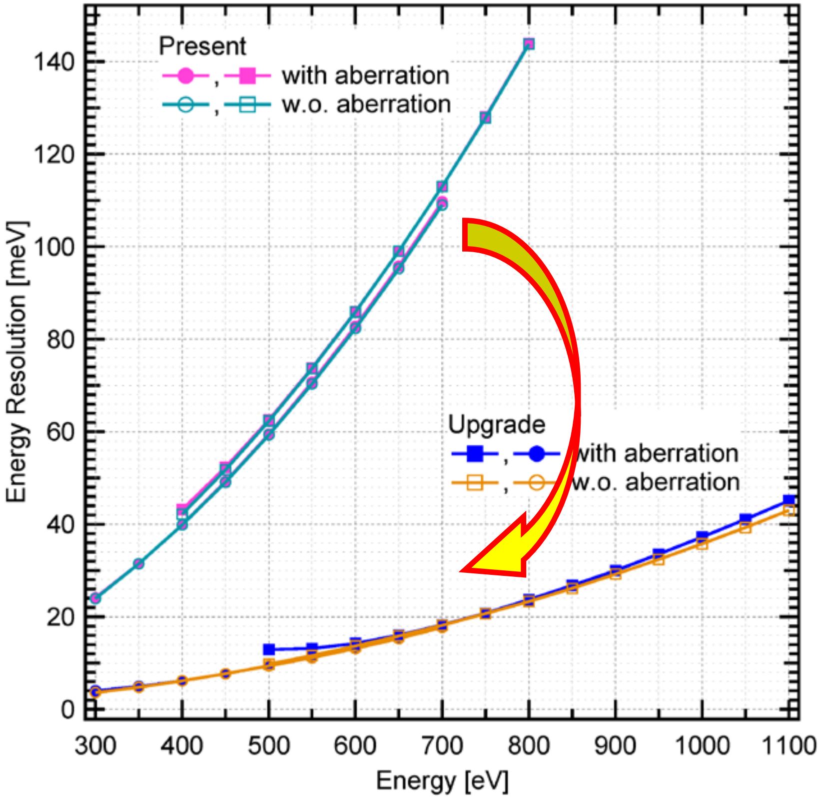

By upgrading the refocusing mirrors, grating of HORNET, and CCD,
the energy resolution is improved more than **five times**
with keeping the present detection efficiency.
Since the flux at the sample position is expected to be increased
more than ten times, the efficiency will significantly be enhanced.

Ultrahigh Resolution RIXS

Beamline

Maximum length of RIXS spectrometer is **~12m**.

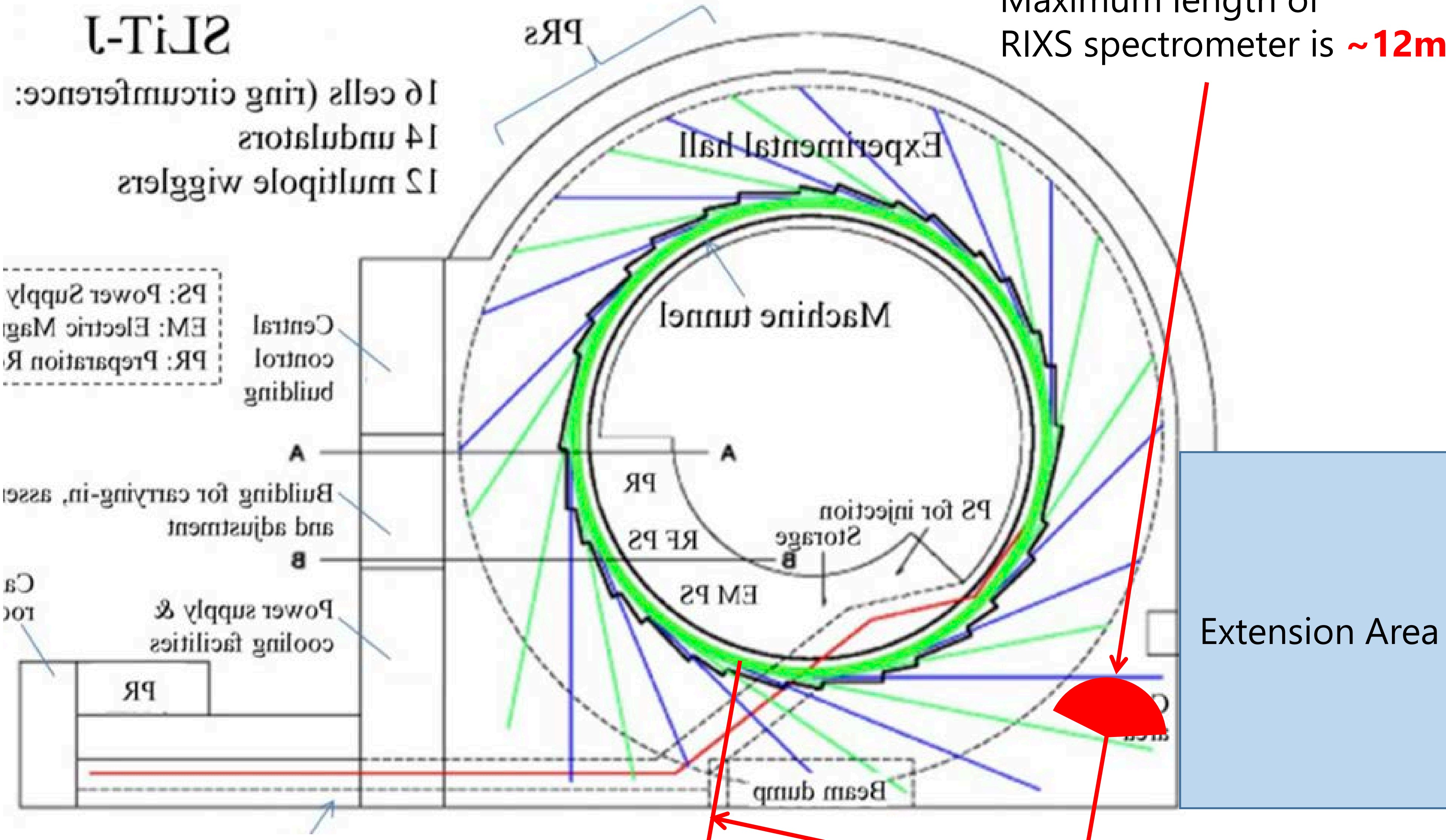

Distance from source to sample is **~76m.**

Optical Layout of Beamline

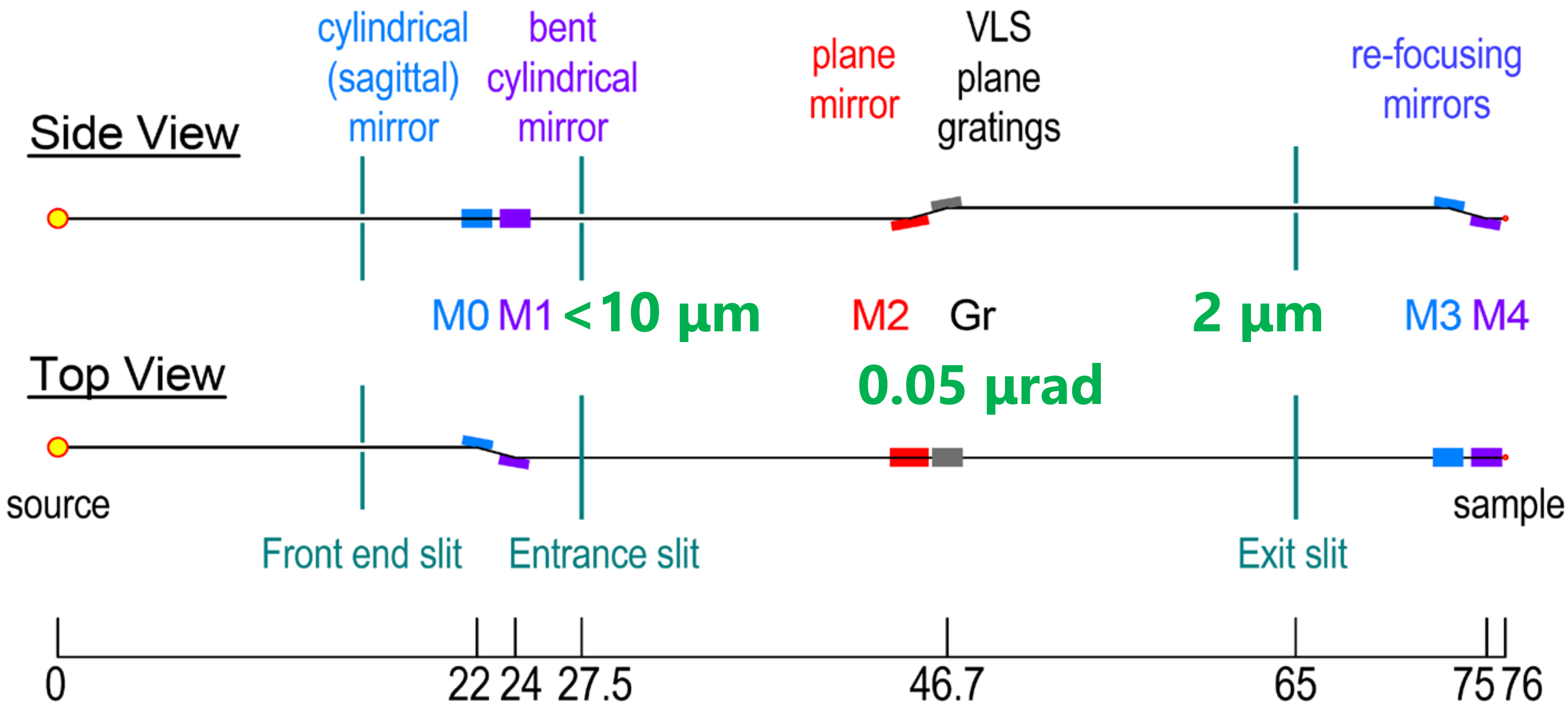

The beamline optics were designed within ~76 m total length.
The included angle of grating and groove parameters were determined by minimizing the aberrations, partially considering the reflectivity, diffraction efficiency, and heat load.

Resolution

Parameters of beamline grating.

	LE	HE
Energy Range (eV)	200–600	500–1500
a_0 (l/mm)	1800	2000
a_1 (l/mm^2)	0.203825	0.236512
a_2 (l/mm^3)	1.59681×10^{-5}	1.78836×10^{-5}
Entrance slit (μm)	<10	
Exit slit (μm)	2	
Slope Error (μrad in rms)	0.05	
Length of grating (mm)	250	

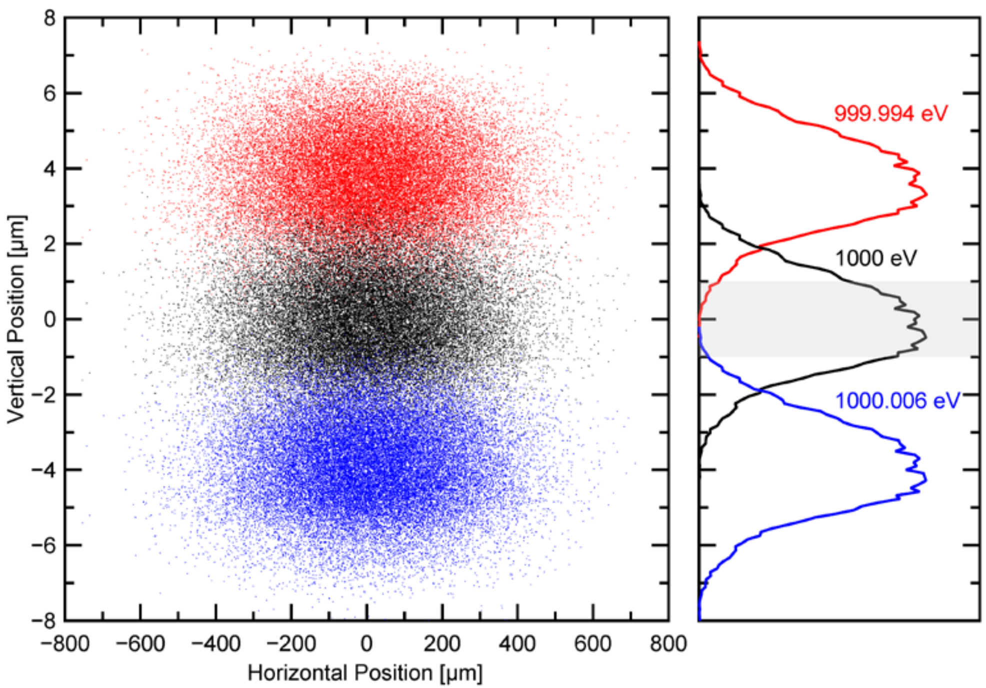

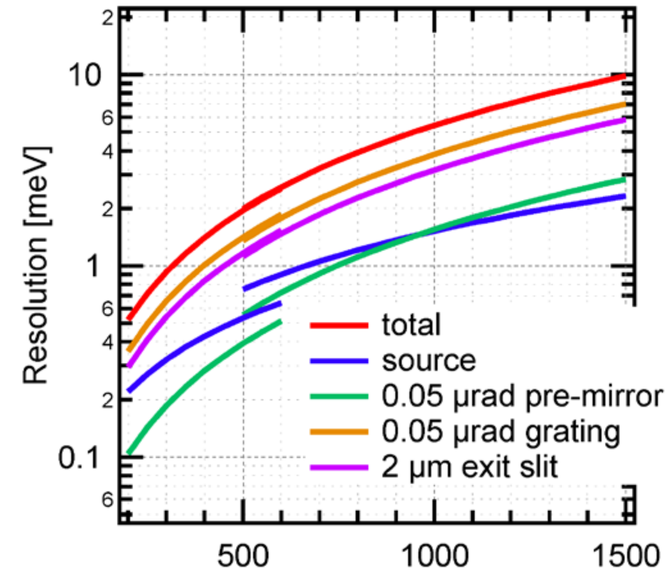

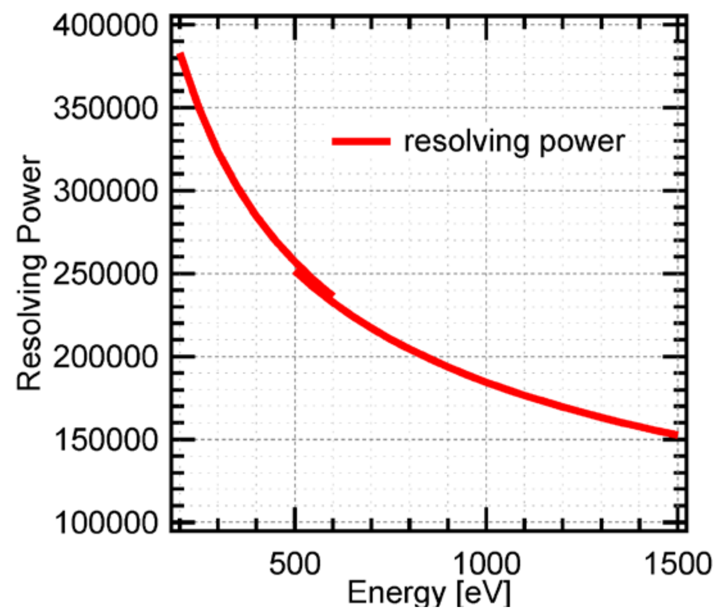

Optical Design of RIXS Spctrometer

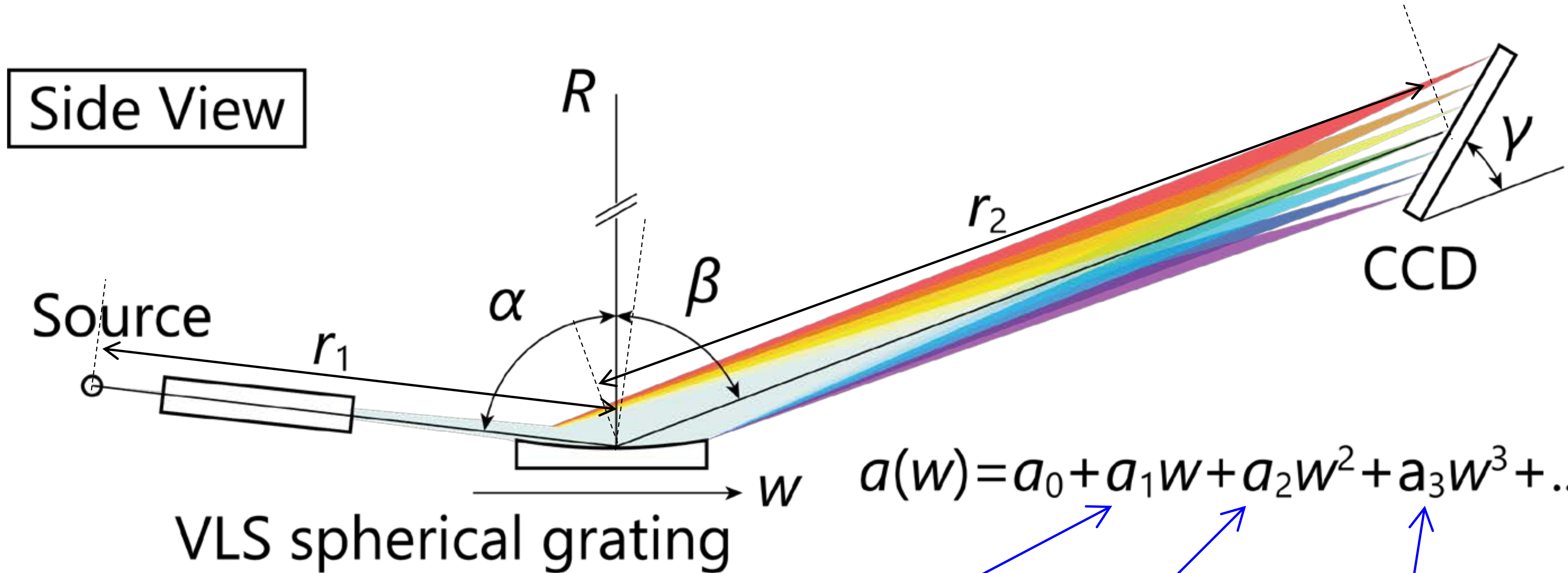

$$a(w)=a_0+a_1w+a_2w^2+a_3w^3+\ldots$$

Focal distance &
focal curve inclination
(in combination with R)

Cancelation of
coma aberration

Compensation for
higher order aberration
(large grating illumination)

- Single optical element
- Ease of operation & alignment
- Constrained VLS parameters optimization

Aberration Free for 500–1000 eV

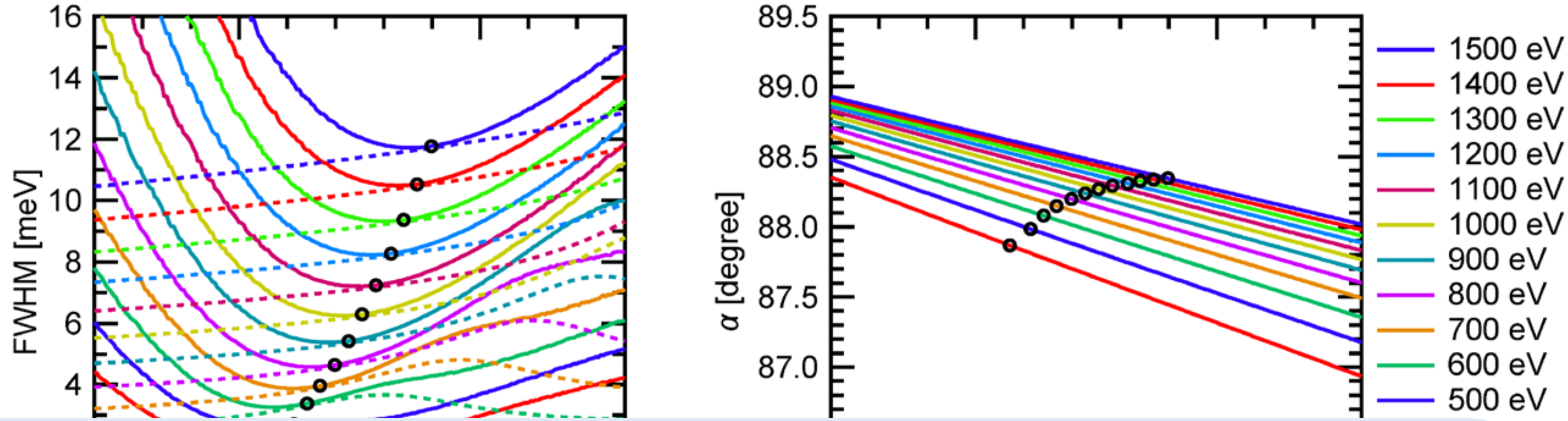

😀 aberration free

😓 large CCD motion range: >2 m for 500–1000 eV

😓 large γ motion range: 20–80° for 500–1000 eV

😓 low energy resolution at lower energy due to large γ

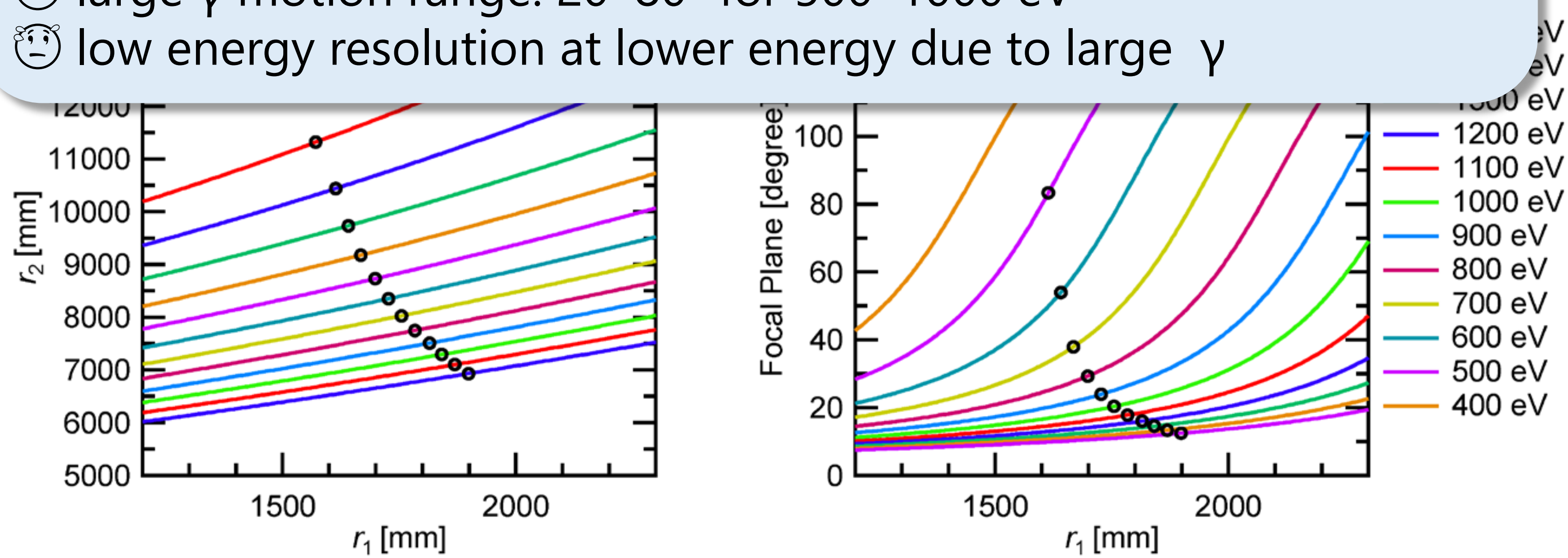

Optimization of Parameters

Under the condition that $L = r_1 + r_2 = 12$ m,
$\Delta_S = 0.5$ μm, $\Delta_{SE} = 0.05$ μrad in rms, and $\Delta_E = 2$ μm,
other parameters are optimized at an energy E_0.

	LE	HE
Energy range (eV)	200–450	400–1000
E_0 (eV)	200	400
Radius of curvature (mm)	148969	122589
a_0 (l/mm)	2000	2600
a_1 (l/mm^2)	0.255216	0.282063
a_2 (l/mm^3)	1.45790×10^{-5}	-6.76584×10^{-5}
a_3 (l/mm^4)	2.01544×10^{-8}	8.90093×10^{-8}
Vertical spot size (μm)	0.5	
Spatial resolution of CCD (μm)	2	
γ (degree)	20–40	
Slope error (μrad in rms)	0.05	
Length of grating (mm)	250	200

Aberration Free & Constant FP

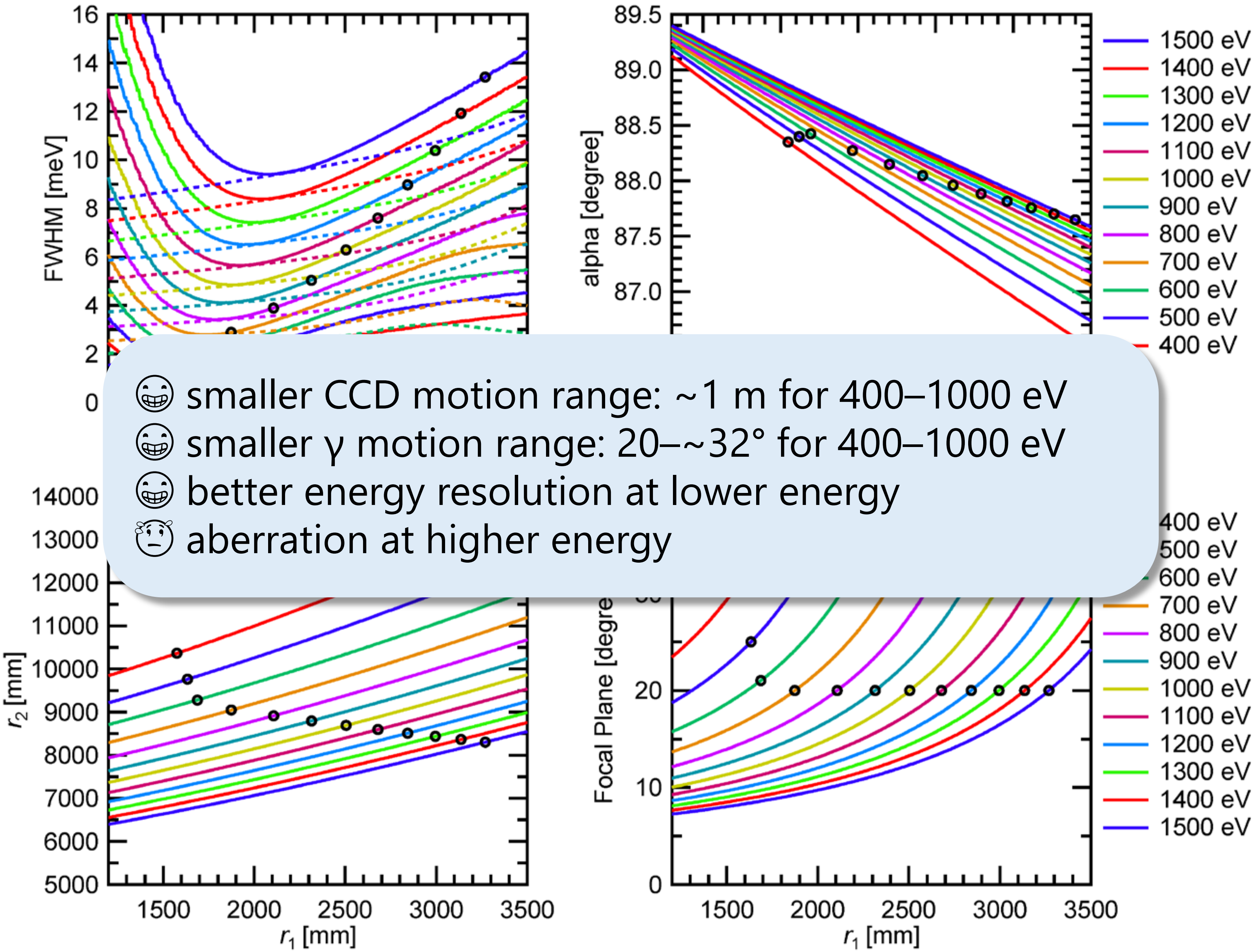

- 😁 smaller CCD motion range: ~1 m for 400–1000 eV
- 😁 smaller γ motion range: 20–~32° for 400–1000 eV
- 😁 better energy resolution at lower energy
- 😓 aberration at higher energy

Aberration Free & Constant FP

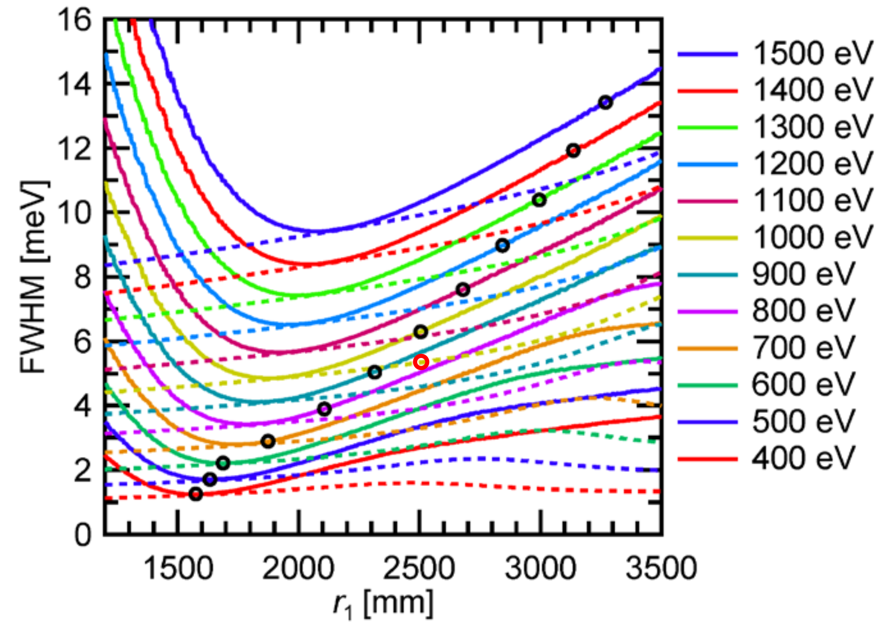

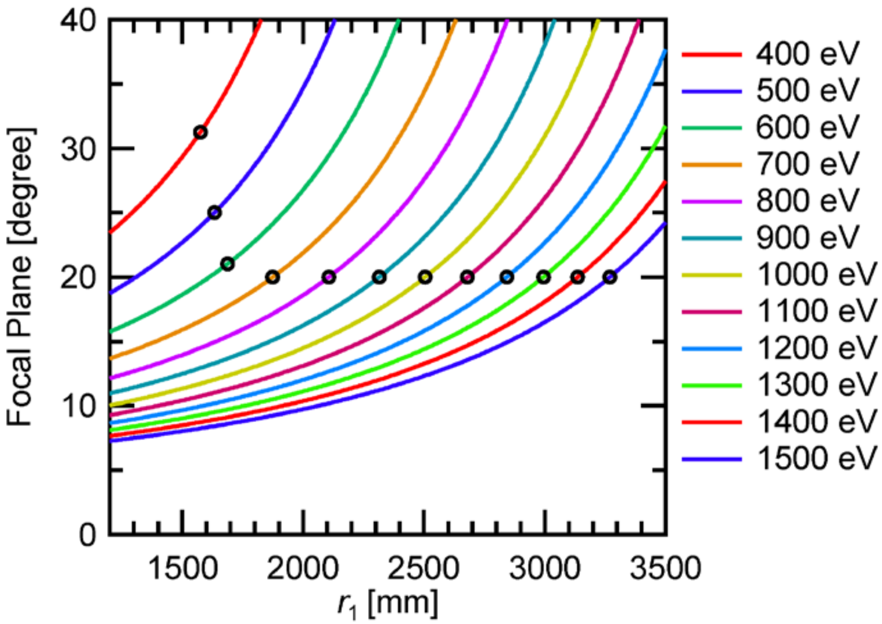

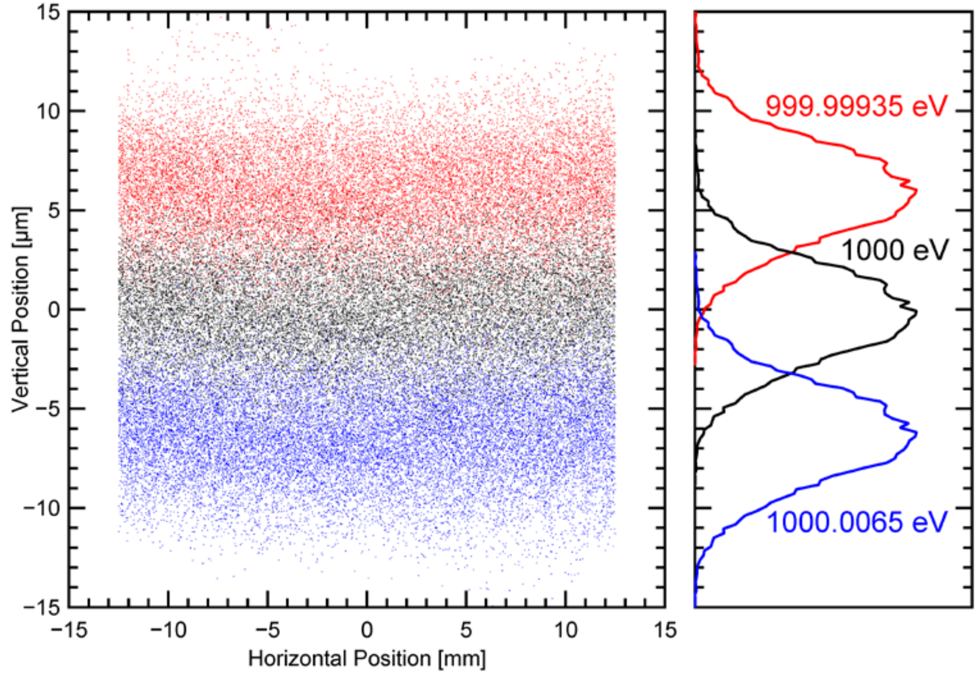

The focusing profile is symmetric, although the aberrations degrade the energy resolution

Requirements for Meachanical Motion

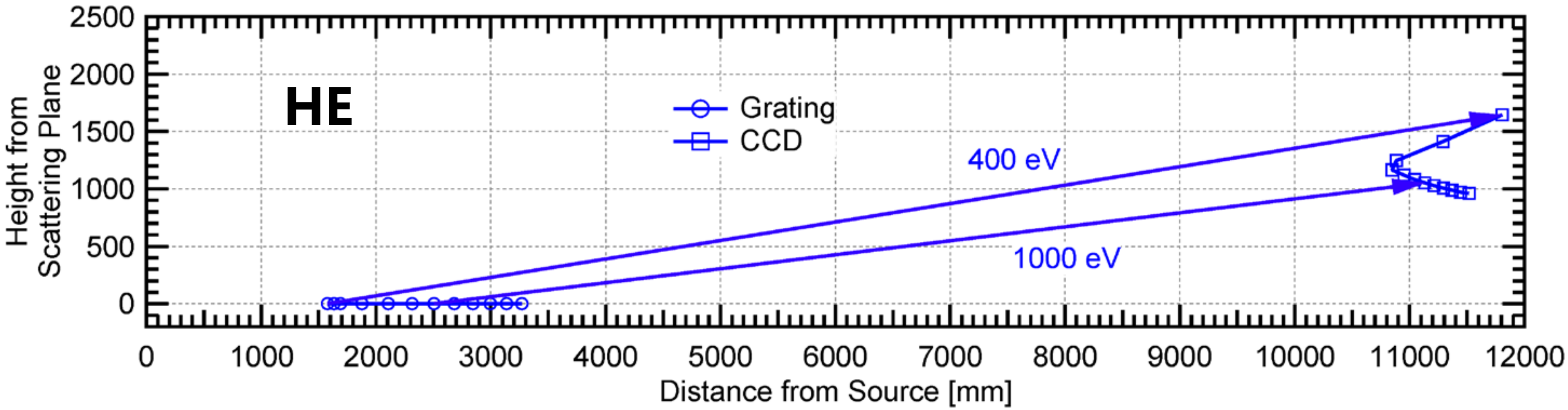

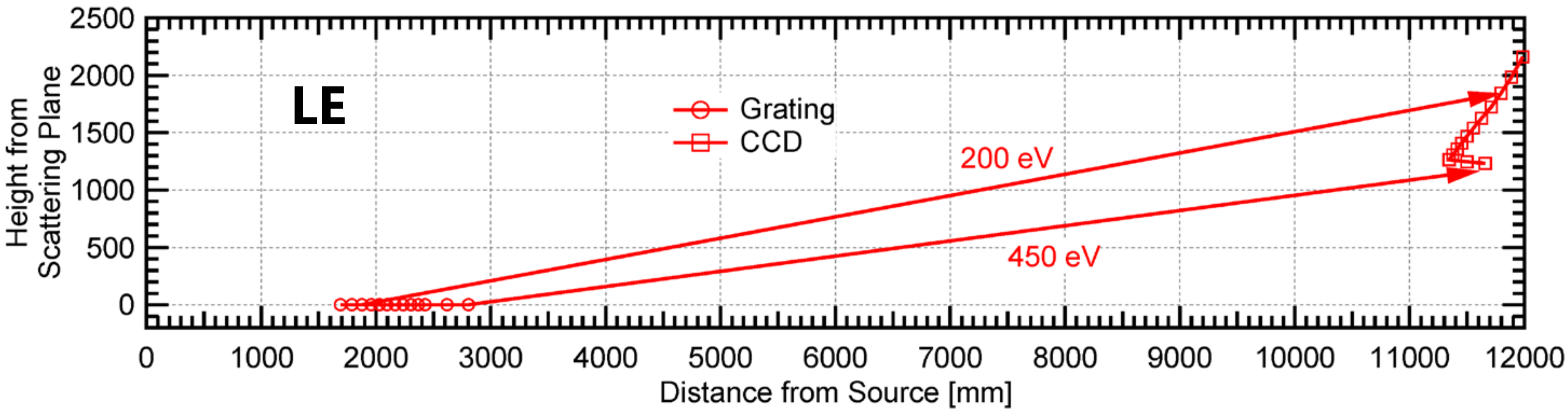

Motion ranges required for grating and CCD are moderate, but ~20° motion of CCD angle γ is required.

Total Resolving Power

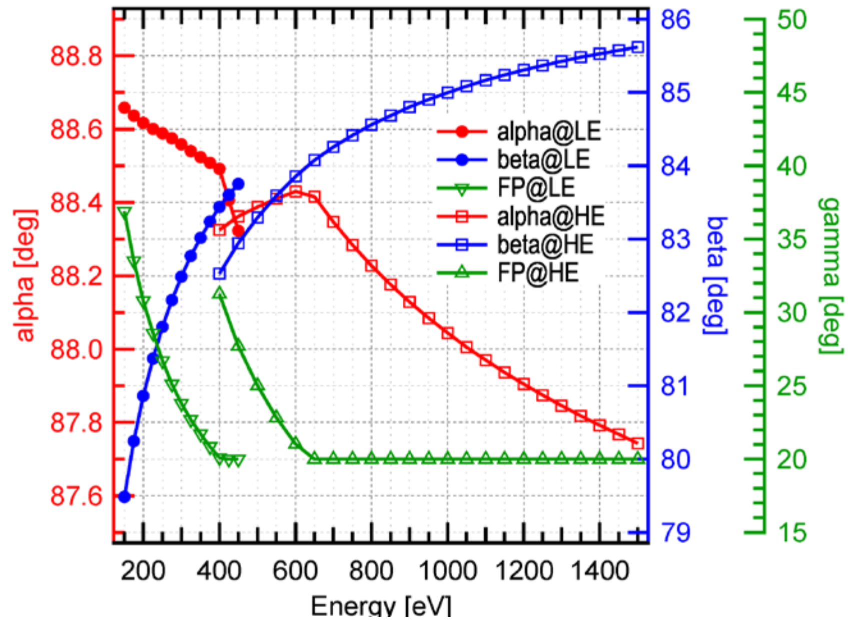

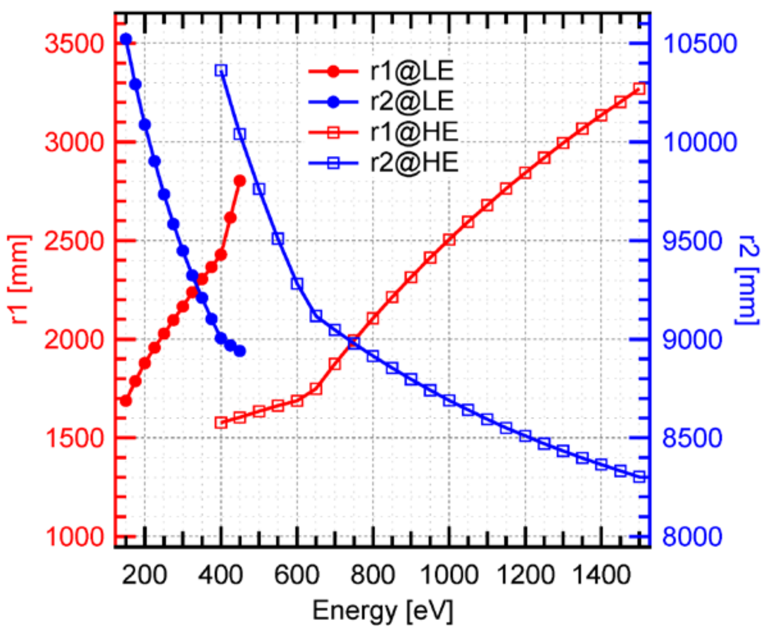

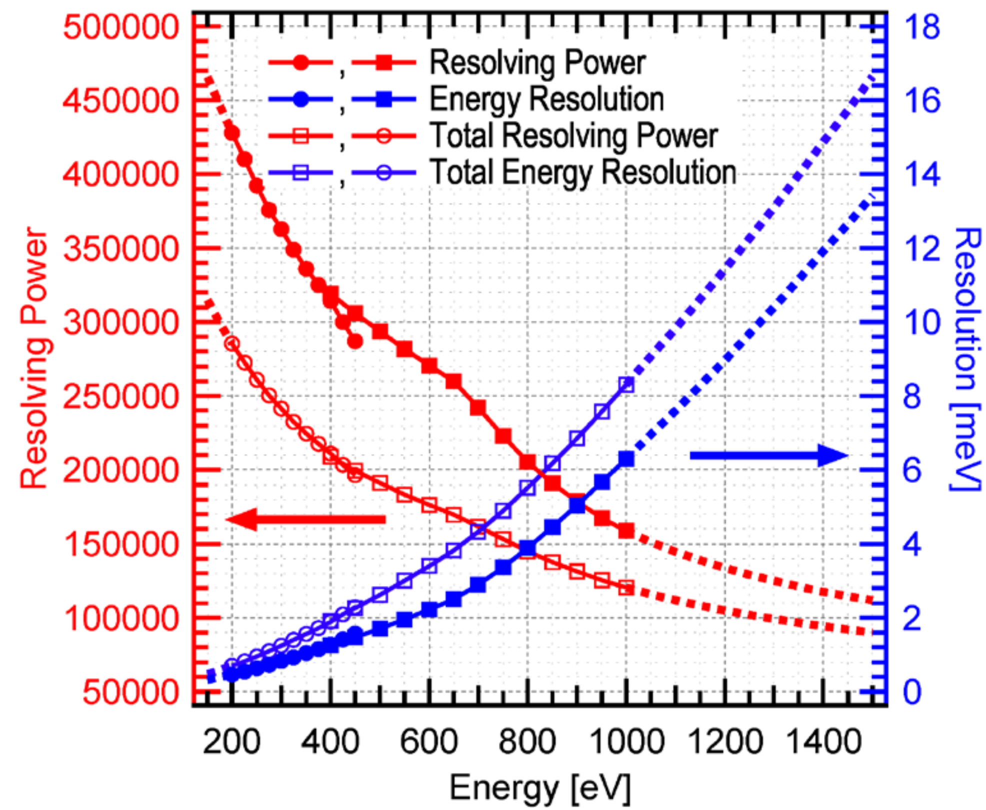

To achieve single-meV resolution
in total length of ~12 m,
Δ_S=0.5 µm, Δ_{SE}=0.05 µrad, and Δ_D=2 µm
are required.

Resolving Power

Δ_S=0.5 μm, Δ_{SE}=0.05 μrad

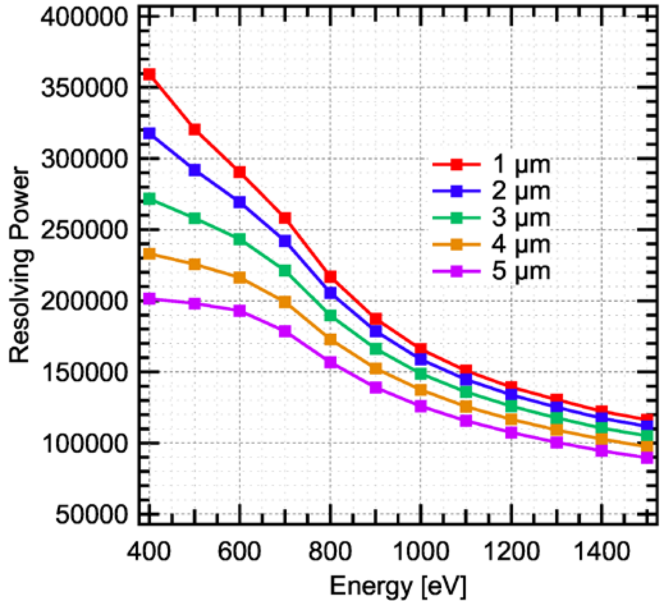

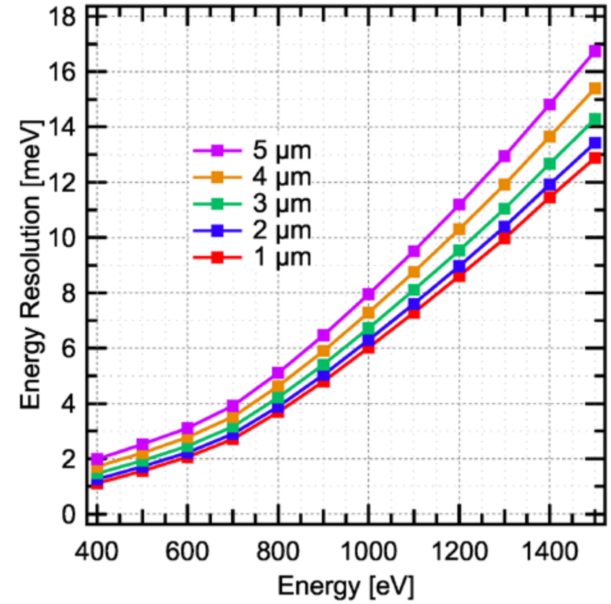

Δ_S=0.5 μm, Δ_D=2 μm

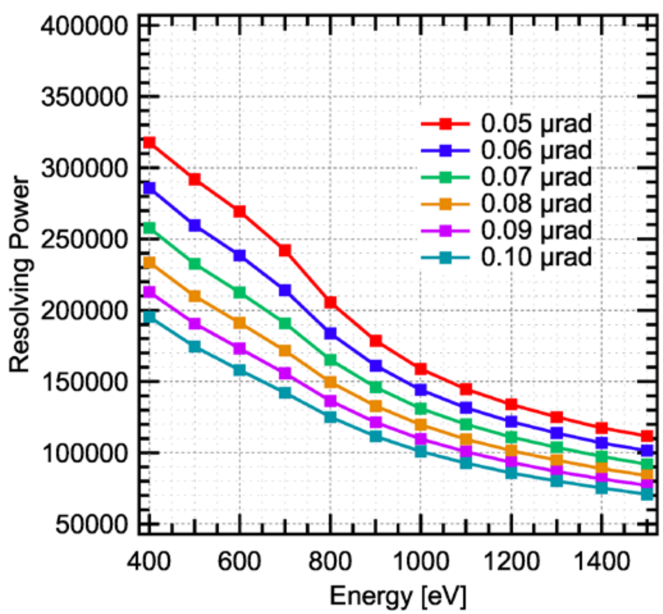

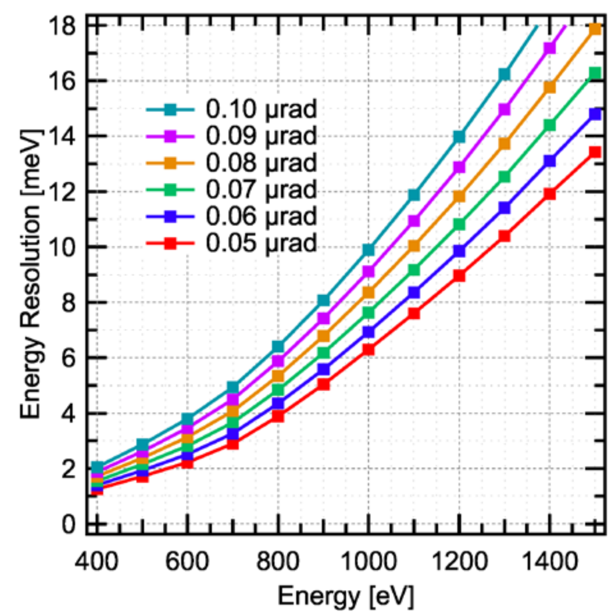

Summary

- A compact permanent-magnet system is available at HORNET in SPring-8 BL07LSU for facile studies of magnetic dichroism in RIXS. RIXS-MCD has been applied to several samples, and unique results are now on publish.
- Ultrahigh efficiency and ultrahigh resolution RIXS spectrometers, and an ultrahigh resolution soft X-ray beamline were designed.
- Ultrahigh efficiency RIXS spectrometer can be realized using HORNET at SPring-8. The efficiency will be improved more than 10 times thanks to the increase of the flux at the sample position, and the energy resolution will become more than 5 times better by upgrading refocusing mirrors, grating, and CCD.
- The feasibility of single-meV resolution SX-RIXS beamline and spectrometer was examined. The reflectivity, diffraction efficiency, and heat load were partially considered, but full optimization including these will be performed.

Acknowledgements

- RIXS-MCD

F. Kuroda, H. Fujii, T. Oguchi, S. Suga *ISIR, Osaka Univ.*

H. Fujiwara, K. Nagai, Y. Nakatani,
M.kawada, A. Sekiyama *Grad. Sch. of Eng. Sci., Osaka Univ.*

R. Y. Umetsu *Tohoku Univ.*

M. Urasaki, H. Ikeno *Osaka Pref. Univ.*

H. Niwa *Tsukuba Univ.*
H. Kiuchi *Kyoto Univ.*
Y. Harada *ISSP, Univ. of Tokyo*

- Optical design of beamline

K. Amemiya *KEK-PF*

Thank you for your attention!